

Purification, Characterization, and Preliminary Crystallographic Study of Copper-Containing Nitrous Oxide Reductase from *Pseudomonas nautica* 617[†]

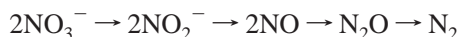
Miguel Prudêncio,[‡] Alice S. Pereira,[‡] Pedro Tavares,[‡] Stéphane Besson,[‡] Inês Cabrito,[‡] Kieron Brown,[§] Bart Samyn,^{||} Bart Devreese,^{||} Jozef Van Beeumen,^{||} Frank Rusnak,[⊥] Guy Fauque,[#] José J. G. Moura,[‡] Mariella Tegoni,[§] Christian Cambillau,[§] and Isabel Moura^{*.‡}

Departamento de Química, CQFB, Faculdade de Ciências e Tecnologia, Universidade Nova de Lisboa, 2825-114 Caparica, Portugal, Architecture et Fonction des Macromolécules Biologiques, URA 9039, CNRS, 31 Chemin Joseph Aiguier, 13402 Marseille Cedex 20, France, Laboratory of Protein Biochemistry and Protein Engineering, University of Gent, K.L. Ledeganckstraat 35, 9000 Gent, Belgium, Department of Biochemistry and Molecular Biology, Mayo Clinic Foundation, Rochester, Minnesota 55905, and Laboratoire d'Océanographie et de Biogéochimie, Centre d'Océanologie de Marseille (OSU), Université de la Méditerranée, UMR CNRS 6535, Campus de Luminy—Case 901, 13288 Marseille Cedex 09, France

Received November 15, 1999; Revised Manuscript Received January 20, 2000

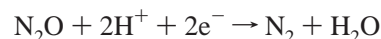
ABSTRACT: The aerobic purification of *Pseudomonas nautica* 617 nitrous oxide reductase yielded two forms of the enzyme exhibiting different chromatographic behaviors. The protein contains six copper atoms per monomer, arranged in two centers named Cu_A and Cu_Z. Cu_Z could be neither oxidized nor further reduced under our experimental conditions, and exhibits a 4-line EPR spectrum ($g_x = 2.015$, $A_x = 1.5$ mT, $g_y = 2.071$, $A_y = 2$ mT, $g_z = 2.138$, $A_z = 7$ mT) and a strong absorption at ~640 nm. Cu_A can be stabilized in a reduced EPR-silent state and in an oxidized state with a typical 7-line EPR spectrum ($g_x = g_y = 2.021$, $A_x = A_y = 0$ mT, $g_z = 2.178$, $A_z = 4$ mT) and absorption bands at 480, 540, and ~800 nm. The difference between the two purified forms of nitrous oxide reductase is interpreted as a difference in the oxidation state of the Cu_A center. In form A, Cu_A is predominantly oxidized ($S = 1/2$, Cu^{1.5+}–Cu^{1.5+}), while in form B it is mostly in the one-electron reduced state ($S = 0$, Cu¹⁺–Cu¹⁺). In both forms, Cu_Z remains reduced ($S = 1/2$). Complete crystallographic data at 2.4 Å indicate that Cu_A is a binuclear site (similar to the site found in cytochrome *c* oxidase) and Cu_Z is a novel tetracopper cluster [Brown, K., et al. (2000) *Nat. Struct. Biol.* (in press)]. The complete amino acid sequence of the enzyme was determined and comparisons made with sequences of other nitrous oxide reductases, emphasizing the coordination of the centers. A 10.3 kDa peptide copurified with both forms of nitrous oxide reductase shows strong homology with proteins of the heat-shock GroES chaperonin family.

Denitrification constitutes one of the main branches of the global nitrogen cycle. In this process, nitrate is reduced to dinitrogen through the series of reactions outlined below.



This respiratory process is coupled to ATP generation. The enzymes involved in denitrification are usually synthesized under anaerobic conditions in the presence of nitrogen oxides, although denitrification can also occur in the presence of

oxygen (1, 2). Many denitrifying bacteria grow at the expense of N₂O as the sole electron acceptor for the oxidation of organic compounds (3). Nitrous oxide reductase (N₂OR)¹ catalyzes the conversion of N₂O to N₂, the last step of the complete denitrification pathway in denitrifying bacteria. The reaction catalyzed by N₂OR is



N₂OR has been purified from various microorganisms: *Pseudomonas* (*Ps.*) *stutzeri* (formerly *Ps. perfectomarina*) (4), *Rhodobacter capsulatus* (formerly *Rhodopseudomonas capsulata*) (5), *Rhodobacter sphaeroides* f. sp. *denitrificans* (6), *Paracoccus denitrificans* (7), *Wolinella succinogenes* (8), *Achromobacter cycloclastes* (9), *Ps. aeruginosa* (10), *Thiosphaera pantotropha* (11), *Thiobacillus denitrificans* (12), and *Achromobacter xylosoxidans* (13). While these N₂ORs are soluble proteins, a membrane-bound enzyme was detected in the gliding soil bacterium *Flexibacter canadensis*

[†] This work was performed with the financial support of the EU BIOTECH Structural Biology Project (BIO4 CT96-0281), the Foundation for Science and Technology of the Portuguese Ministry of Science and Technology (Program PRAXIS XXI), and the Fund for Scientific Research—Flanders (Programs G.0054.97 and G.0422.98). M.P., S.B., and I.C. are indebted to PRAXIS XXI for research fellowships.

* To whom correspondence should be addressed at the Departamento de Química, CQFB, Faculdade de Ciências e Tecnologia, Universidade Nova de Lisboa, 2825-114 Caparica, Portugal. Telephone: + 351 21 2948381. E-mail: isa@dq.fct.unl.pt.

[‡] Universidade Nova de Lisboa.

[§] AFMB Marseille.

^{||} University of Gent.

[⊥] Mayo Clinic Foundation.

[#] Centre d'Océanologie de Marseille.

¹ Abbreviations: N₂OR, nitrous oxide reductase; COX, cytochrome *c* oxidase; EPR, electron paramagnetic resonance; LT-MCD, low-temperature magnetic circular dichroism; PCR, polymerase chain reaction.

(14). With the exception of N₂ORs from *Rhodobacter sphaeroides*, which contains zinc and nickel (6), and from *Wolinella succinogenes*, which is a heme-copper protein (8), all other purified N₂ORs contain only copper cofactors. Copper N₂ORs exist in several forms, distinguished by their redox and spectroscopic properties and by their enzymatic activity, for which numbers and trivial names are commonly used as reviewed in (3).

The most widely used model regards the copper sites of N₂OR as two binuclear centers: Cu_A and Cu_Z. Cu_A, responsible for the electron transfer from an external donor to the catalytic center (15), is spectroscopically and structurally similar to the Cu_A center of cytochrome *c* oxidase (COX) (16–20). The structure of this latter center was determined (21–25), and its characteristics are reported in a recent review by Beinert (26). Cu_Z is believed to be the catalytic center where N₂O reduction occurs, and its binuclear nature was assumed from chemical analysis and spectroscopic studies [see (3) for a review]. Another, more recent, model considers Cu_A and Cu_Z as variants of the same binuclear copper center, the catalytic center being undetectable by visible or EPR spectroscopies (27). This model, based on results from UV-visible, MCD, and EPR spectroscopies, makes way for speculation as to the possible nature of the catalytic center.

In this manuscript we report the purification, crystallization, and biochemical and spectroscopic characterization of two forms of N₂OR isolated from the halophilic denitrifier *Ps. nautica* 617. These two forms, called A and B, differ in their spectroscopic and redox properties. The gene sequence coding for N₂OR and the deduced amino acid sequence are also presented. The X-ray data have demonstrated that the two copper centers of N₂OR have different features: Cu_A is a binuclear copper center similar to the one found in COX, and Cu_Z, the putative catalytic site, is a novel tetranuclear copper center never before found in biological systems (28). Based on the data presented in this manuscript, we propose a model in which the two purified forms A and B correspond to two different oxidation states of Cu_A, with Cu_Z remaining redox-inactive under our experimental conditions.

EXPERIMENTAL PROCEDURES

Growth of *Ps. nautica* and N₂OR Purification. The reclassification of the type strain of *Pseudomonas nautica* as *Marinobacter hydrocarbonoclasticus* has been proposed (29). However, strain 617 awaits classification, and we will continue to refer to it as *Ps. nautica* 617 to avoid confusion. Three 200 L batches of *Ps. nautica* 617 (Pasteur Institute Collection, ref. *Ps. nautica* no. 617/1.85) were grown under denitrifying conditions in artificial seawater at 30 °C with 10 mM nitrate as electron acceptor (30). Yeast extract (0.1%) and lactate (1%) were used as carbon and energy sources. The medium was supplemented with a separately sterilized Starkey oligoelement solution (31) (0.2 mL/L of culture). Cells were harvested in the late exponential phase of growth by centrifugation. Approximately 600 g of cells (wet paste) was resuspended in 100 mM Tris-HCl, pH 7.0, and broken in a French press. The crude extract was centrifuged at 8000g for 20 min and twice at 12500g for 1 h to remove cell debris and membranes. The resulting supernatant was used for N₂OR purification. To avoid freeze-thaw cycles in intermediate

purification fractions, all steps were carried out nonstop at 4 °C until the protein was considered to be pure. The soluble extract was applied to an anion exchange DEAE-Biogel column (4.5 × 40 cm, Bio-Rad) equilibrated with 10 mM Tris-HCl, pH 7.6. A 10–400 mM Tris-HCl, pH 7.6, linear gradient was applied, and N₂OR-containing fraction eluted at 100–125 mM Tris-HCl. This fraction was loaded onto a Superdex 75 column for gel filtration (2.6 × 56 cm, Pharmacia) run with 300 mM Tris-HCl, pH 7.6. After dialysis, the N₂OR-containing fraction was applied to a Source 15Q anion exchange column (1.6 × 25 cm, Pharmacia) equilibrated with 10 mM Tris-HCl, pH 7.6. A 10–500 mM Tris-HCl, pH 7.6, gradient was applied, and forms A and B of N₂OR were eluted successively between 160 and 200 mM Tris-HCl, pH 7.6. The final yield was approximately 135 mg of total enzyme (A + B).

Analytical Methods. SDS-PAGE electrophoresis was performed with the discontinuous buffer system of Laemmli at 12.5% (32). Native molecular weight determination by gel filtration was performed on a prepacked Superdex 200 HR 10/30 column (Pharmacia). Elution buffer was 50 mM potassium phosphate buffer, pH 7.0, containing 150 mM NaCl. The flow rate was 0.5 mL/min, and 200 μL of protein or standard was injected. The molecular mass standards were ferritin (440 kDa, Pharmacia), catalase (232 kDa, Pharmacia), aldolase (158 kDa, Pharmacia), bovine serum albumin (67 kDa, Sigma), ovalbumin (43 kDa, Sigma), chymotrypsinogen A (25 kDa, Pharmacia), and ribonuclease A (13.7 kDa, Pharmacia). Protein concentration was determined by the method of Lowry et al. (33). Copper content was routinely estimated using the method described by Poillon and Dawson (34). Inductively coupled plasma emission analysis (ICP), performed at the University of Georgia, was also used for copper content determination as well as to investigate the presence of other metals in the enzyme. N₂OR activity was determined spectrophotometrically, at 25 °C, by following the oxidation of reduced methyl viologen at 600 nm under anaerobic conditions (35, 13). The stock solution of enzyme was 125–180 μM. The reaction was performed in 50 mM phosphate buffer, pH 7.1, and was initiated by addition of N₂O-saturated water. N₂OR specific activity is expressed as micromoles of N₂O reduced per minute per milligram of enzyme. Poly(vinylidene difluoride) protein sequencing membranes were used for electroblotting, and N-terminal sequencing was performed on a 476 Sequenator (Perkin-Elmer, Applied Biosystems Division, Foster City, CA). C-terminal sequence analysis was performed on a Procise 494C sequencer (Perkin-Elmer, Applied Biosystems Division) using a chemical procedure slightly modified from the one described in (36). The alkylated thiohydantoin were identified on-line by reversed-phase analysis on a 140C microgradient system, from the same firm, using a linear gradient made from 3.5% tetrahydrofuran/35 mM sodium acetate, pH 3.8, as solvent A, and 100% acetonitrile as solvent B. Prior to sequence analysis, the protein was adsorbed on a ProSorb sample preparation cartridge and, after several subsequent washes with water, treated with phenylisothiocyanate to modify the lysine chains (37). Electrospray mass spectrometry was performed on a Bio-Q quadrupole mass spectrometer equipped with an electrospray ionization source (Micromass, Altrincham, U.K.) as used in (38).

Molecular Biology. *Ps. nautica* cells were grown as previously described. Genomic DNA was isolated using a standard phenol–chloroform extraction protocol (39, 40). The full N₂OR encoding gene was amplified by PCR using two sets of oligonucleotide primers. In the first reaction, a degenerate primer, 5′-GARTACTACGGCTTCTGG-3′, representing the gene sequence of the first residues of the N-terminus was used as the forward primer, while an analogous degenerate primer was designed according to homologies with other N₂OR amino acid sequences (5′-GATGTCGATCARYTGGTCRITC-3′) and used as the reverse primer, resulting in the amplification of a DNA fragment of approximately 1300 bp. To amplify the remaining 550 bp of the N₂OR gene, a second PCR was performed with the following oligonucleotide primers: 5′-GTCCAAGT-TCTCGAAAGACCG-3′ (forward) and 5′-CATSCGRCCSAC-CATYTCCAT-3′ (reverse). In both PCR reactions, ≈50 ng of genomic DNA, ≈50 pmol of each primer, 2.5 mM of each dNTP, and 5 units of *taq* DNA polymerase in 1×PCR buffer (Amersham Pharmacia Biotech) were used in a total volume of 50 μL. The reactions were performed in a thermal cycler (Biometra) using the following program: 1 cycle at 94 °C for 5 min, followed by 35 cycles of 0.5 min at 94 °C, 1.5 min at 56 °C, 2 min at 72 °C, and a final extension step for 10 min at 72 °C. The PCR products were analyzed by electrophoresis in a 0.8% agarose gel in the presence of ethidium bromide using 1×TAE buffer. The fragments of interest were purified from contaminants by gel extraction using the QIAquick Gel Extraction Kit (QIAGEN) and subsequently ligated into the commercial pGEM-Teasy vector from Promega according to the manufacturer's instructions. The resulting DNA plasmids were transformed into Epicurian Coli XL1-Blue competent cells (Stratagene) which were grown overnight in Luria Broth medium with 100 μg/mL ampicillin at 37 °C. Positive recombinant clones were screened after their white color and confirmed by restriction digestion analysis of plasmidic DNA with *NotI*. Plasmidic DNA from single transformants was isolated using the Wizard *Plus* Minipreps DNA Purification System (Promega) and sequenced at the Mayo Clinic Molecular Biology Facility.

Protein Crystallization. Purified N₂OR (form B) from *Ps. nautica* was concentrated to 5 mg/mL in a buffer solution of 100 mM Tris-HCl, pH 7.6. Crystals were obtained by the technique of vapor diffusion at 20 °C with hanging drops of 3 μL of protein solution, mixed with 3 μL of reservoir solution containing typically 18% PEG 4000, 0.1 M BICINE, 0.6 M NaCl, 15% 2-propanol, 10 mM spermine·4HCl at a final pH of 9.5. X-ray diffraction data were collected on BM14 (ESRF). The three-dimensional structure solved by the MAD (multiple wavelength anomalous dispersion) technique at 2.4 Å will be described elsewhere (28).

Spectroscopic Measurements. UV–visible spectra of enzyme solutions were recorded on either a Shimadzu UV-160A or a Shimadzu UV-265FS spectrophotometer. The crystal visible spectra were recorded with the ORIEL microspectrophotometer on ID09 beamline (ESRF), using unpolarized light. The crystals were taken from the mother liquor, transferred for a few seconds to the cryo-cooling solution (10% ethylene glycol), mounted on a cryo-loop, and flash-frozen to 100 K in a cold stream of nitrogen gas (Oxford Cryosystems). Care was taken to record optical

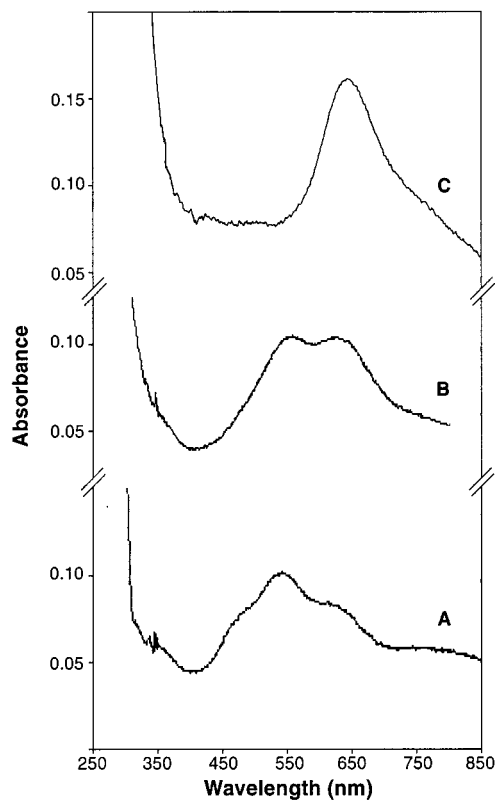


FIGURE 1: UV–visible spectra of *Ps. nautica* N₂OR. (A) Form A; (B) form B; and (C) dithionite-reduced enzyme.

densities in the linearity range (OD < 2.5). The dark current corresponding to electronic noise was measured, and the base line correction was performed with the buffer in which the crystals were soaked. EPR measurements were performed on an X-band Bruker EMX spectrometer equipped with a dual-mode cavity (model ER4116DM) and an Oxford Instruments continuous-flow cryostat. EPR spectra were simulated using the program WINEPR–SimFonia (Bruker). Spin quantitations were made by double integration of a signal obtained under nonsaturating conditions and comparison to a Cu(II)–EDTA standard.

Redox Titrations. Redox titrations of N₂OR were performed anaerobically in 100 mM Tris-HCl, pH 7.6, at 20 °C. A mixture of 16 mediators covering redox potentials ranging from –550 to +430 mV, each at the final concentration of 2 μM, was used to facilitate electron transfer during the oxidation and reduction cycles. The mediators used were as follows: triquat, methyl viologen, neutral red, safranin, phenosafranin, anthraquinone-2-sulfonic acid, 2-hydroxy-1,4-naphthoquinone, phenazine, indigo carmine, indigo tetrasulfonate, duroquinone, 5-hydroxy-1,4-naphthoquinone, 1,4-naphthoquinone, 1,2-naphthoquinone, 2,6-dichlorophenol indophenol, and potassium ferricyanide. The protein solution (174 μM) was reduced by addition of aliquots of sodium dithionite (in 100 mM Tris-HCl, pH 9.0) or oxidized with potassium ferricyanide (in 100 mM Tris-HCl, pH 7.6). The potential was monitored by using a platinum electrode as a measuring electrode and a Ag/AgCl electrode as a reference electrode. Calibration was performed with a saturated solution of quinhydrone at pH 7.0. Samples were collected under anaerobic conditions at different potentials, and the spin concentration of each spectrum was plotted against the measured redox potential.

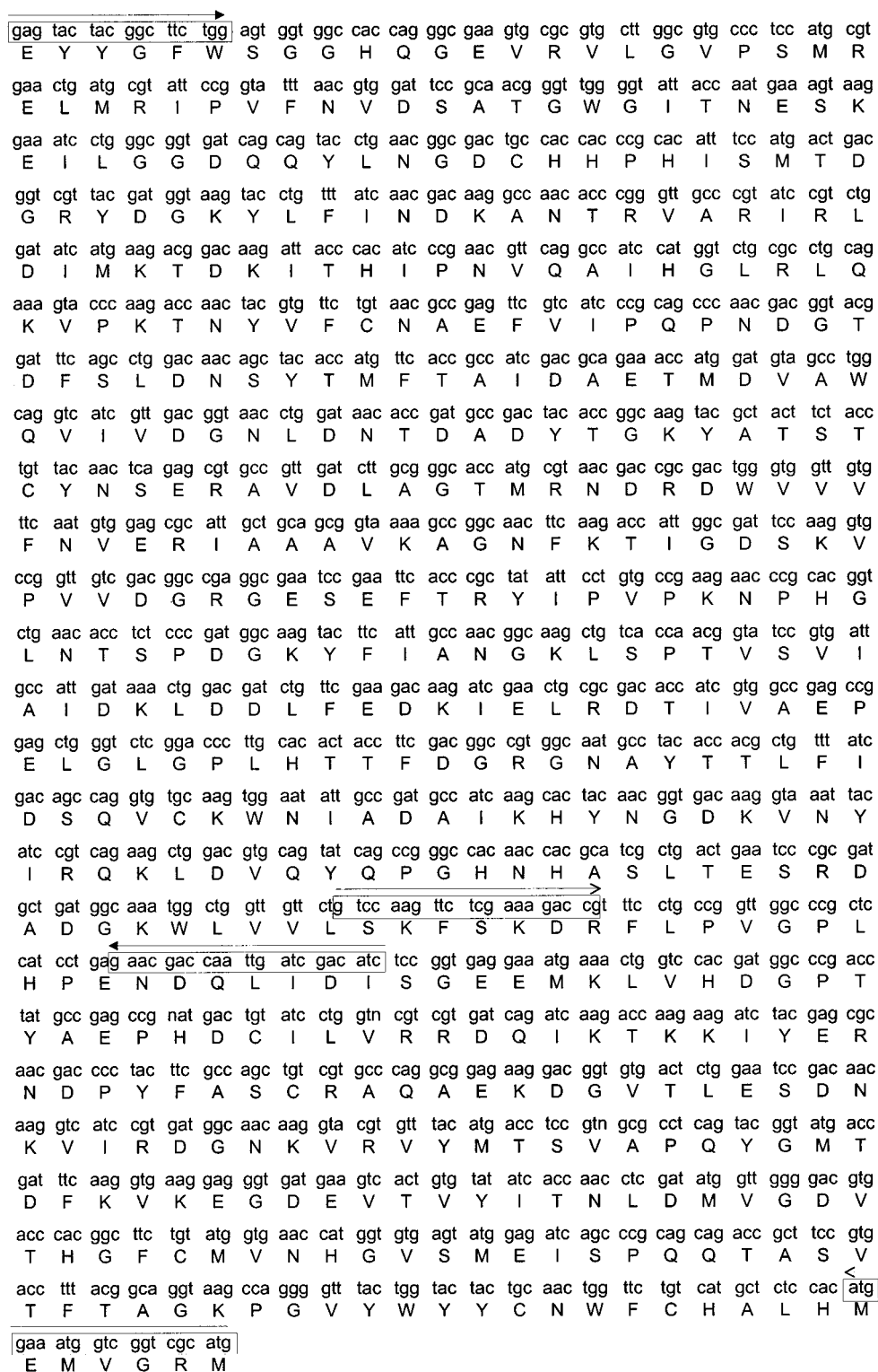


FIGURE 2: DNA and deduced amino acid sequences of *Ps. nautica* N₂OR. PCR oligonucleotide primers are indicated in boxes, and pairs of primers are identified by the type of arrow above the box.

RESULTS

N₂OR Purification. After the first purification step, N₂OR exhibited a purple color, with an intense absorption peak at ~540 nm. However, after the second anion exchange step, a separation was achieved between a predominantly purple form (called A) and a blue-colored form (called B), with different visible spectra (Figure 1A,B). Form B eluted at a slightly higher ionic strength than form A. Both forms were active and exhibited similar specific activities: 55 ± 6 and

23 ± 14 μmol of N₂O reduced·min⁻¹·(mg of enzyme)⁻¹ for forms A and B, respectively. However, maximum specific activity was only achieved with a preincubation of the enzyme with dithionite-reduced methyl viologen. N₂OR was found to be sensitive to dilution. Upon dilution of N₂OR stock solution from 10 to 1 mg/mL, the specific activity decreased with time in an exponential manner to reach the value of approximately 1 μmol of N₂O reduced·min⁻¹·(mg of enzyme)⁻¹ 3 h after dilution. The two forms were

Ps.n.	-----AAEEE-----ARNKAHVAPGEL	17
Ps.s.	MSDKSKNTPOVPEKLGSLRRGFLGASAVT--GAAVAATA---LGGAVMTR--ESWAQAVKE----SKQKIHVGPGE	67
Ps.a.	MSDKQTKD---EKTGLSRRGFLGASALT--RSAVAASG---LVGGVMTR--DSWAAAAKE-----AQQKIHVAPGEL	63
A.c.	MESKEHKG-----LSRRALFSATAGS--AILAGTVG-----PAALSLGAAGLATPARA---ATGADGVSAPGKL	59
Pa.d.	MESKQEKG-----LSRRALLGATAGG--AAVAGAFGRRLLALGPAALGLGTAGVATVAGSAAALASGDGVSAPGQL	69
S.m.	MSNEETKMR-----LNRRQMLGTTA-F--MAAAGAVG-----AGGALTL--SGGTATPARAQ--ETSGSSEYEVKPGEL	61
R.e.	MSKEKASIGN---GPGGIGRRQFLGTAALAGLAGVAVCATDKGAAPAAAAGVAPASGAHGAHG-----AGASVHLKPGEL	72
Ps.n.	DEYYGFWSGGHQGEVRLGVPSMRELMRIPVFNVDSATGWGITNES-----KEILGGDQQYL-----NGDCPHPHI	83
Ps.s.	DDYYGFWSGGHQGEVRLGVPSMRELMRIPVFNVDSATGWGLTNES-----RHIMGDSAKFL-----NGDCPHPHI	133
Ps.a.	DEYYGFWSGGHQGEVRLGVPSMRELMRIPVFNVDSATGWGLTNES-----RHILGDTAKFL-----NGDCPHPHI	129
A.c.	DDYYGFWSGGQTEGEMRILGIPSMRELMRVPVFNRCSATGWGQTNESIRIHQRTMTEKTKKQLAANGKKIHNDGDLHVVHM	139
Pa.d.	DDYYGFWSGGQSGEMRILGIPSMRELMRVPVFNRCSATGWGQTNESVRIHERTMSERTKKFLAANGKRIHDNDGDLHVVHM	149
S.m.	DEYYVFFSSGGQSGEIRIVGAPSMREMRIPVFNRCSATGWGQTNESRKVMTEGLLPETVEFLKDDQG--GLYLNNDLPHPHI	140
R.e.	DTYYGLWSGGHTGDMRVLGLPSGREILRIPCVPFDALVWGITNES-----KKVMGARPDGTLR-----YTVADEPHH	142
Ps.n.	SMTDGRYDGGKYLFINDKANTRVARIRLDIMKTDKITHIPNVQAIHGLRLQK-----VPKTYVFCNAEFVFPQNDGT	156
Ps.s.	SMTDGGKYDGGKYLFINDKANSRVARIRLDIMKCDKMITVFNQAIHGLRLQK-----VPHTKYVFCNAEFVFPNDGT	206
Ps.a.	SMTDGGKYDGGKYLFINDKANSRVARIRLDIMKCDKMITVFNQAIHGLRLQK-----VPHTKYVFCNAEFVFPNDGT	202
A.c.	SFTDGGKYDGRYLFMNDKANTRVARVRCVDMKTDAILIPNAKGIHMRPQK-----WPRSNYVFCNGEDEAPLVNDGS	212
Pa.d.	SFTDGGKYDGRYLFMNDKANTRVARVRCVDMKTDAILIPNAKGIHMRPQK-----WPRSNYVFCNGEDEAPLVNDGT	222
S.m.	SFTDGTYYDGRYLYANDKSNRVRIRLDVIMKCDKIQLPNQHTVHGLRVQK-----YPKTYVFCNGEDEVFPNDGT	213
R.e.	SYKDGNYDGRYAWVNDKINSRIARIRLDYFICDKITELPNVQGFHGFIPDKRDPVDTKINNYTRVFCGGEFGIPLPSAPT	222
Ps.n.	DFSLD--NSYTMFTAIDAETMDVAWQVIVDGNLNDTDADYTGKYATSTCYNSERAVDLAGTMRNDRDWWVFNVERIAAA	234
Ps.s.	VFDLQDENSYTYMYNAIDAETMEMAFQVIVDGNLNDTDADYTGGRFAAATCYNSEKAFDLGGMMRNERDWWVFDIHAVEAA	286
Ps.a.	VFDLEDENSFTMYNAVDAETMEVAFQVIVDGNLNDTDADYTGGRFAAATCYNSEKAFDLGGMMRNERDWWVFDISAVEKE	282
A.c.	TMTDVA--TYVNIFTAVDADKWEVAWQVKVSGNLNDADYEGKWFSTSYNSEKGMTLEEMTKSEMMDHVVFVFNIAEIEKA	291
Pa.d.	NMEDVA--NYVNIFTAVDADKWEVAWQVLSGNLNDADYEGKWFSTSYNSEKGMTLEEMTKSEMMDHVVFVFNIAEIEKA	301
S.m.	TMGDKN--SYQAIFTAVDGETMEVAWQVMVDGNLNDADYQKGYCFATCYNSEGFTLADMMASEQDWWVIFNLKRIEAA	292
R.e.	EDAGK---YRSLFTCVDAETMAVRWQVLIDGNCDLVATSYDGKLAATNQYNTENGAHFEDMMSAERDCAVFFNIARIEAA	299
Ps.n.	VKAGNFKITGDSKVPVVDGRG-----ESEFTRYIPVKNPHEGLNTSPDGKYFIANGKLSPTVSVIAIDKLDLDFEDKI-	307
Ps.s.	VKAGDFITLGDSTKTPVLDGRKDKG--DSKFTRYVVPKNPHEGCNTSSDGKYFIANGKLSPTCSMIAIDKLPDLFAGKLA	364
Ps.a.	IKAGRFITLGDSTKVPVVDGRKDKG--DSVTRYIPVKNPHEGLNTSTDGKYFIANGKLSPTCSMIAIDLPLDFAGKLL	360
A.c.	IKAGQYEEING--VKVVDGRKE--A--KSLFTRYIPIANNPHEGCNMAPDRKHLVAGKLSPTVTLVDVTKFDALFYDNA-	364
Pa.d.	IAAGDYQELNG--VKVVDGRKE--A--SSLFTRYIPIANNPHEGCNMAPDRKHLVAGKLSPTATVLDVTRFDVAVFYENA-	374
S.m.	VAKDYEKIGG--VPVLDGRK-----GSPYTRYVVPVNSPHEGINTAPDGIHVVANGKLSPTVTVFVDRVKFDLDFDDKI-	363
R.e.	VQAGFKTYGDSKVPVVDGTAQANKDPKALTAYVSVKPNPHEGVNASPDQKYFICAGKLSPTATVIELSRVLGVDGKQGE	379
Ps.n.	ELRDTIVAEPELGLGLPHTTDFDGRGNAYTTLFIDSQVCKWNIADAIKHYNGDR-VNYIKQKLDVHYQPGHLSLTSRD	386
Ps.s.	DPRDVIVGEPGLGLPHTTDFDGRGNAYTTLFIDSQVVKWNEEAARAYKGEK-VNYIKQKLDVHYQPGHLSLTSRD	443
Ps.a.	DPRDVIVGEPGLGLPHTTDFDGRGNAYTTLFIDSQVVKWNEEAARAYKGEK-VNYIKQKLDVHYQPGHLSLTSRD	439
A.c.	EPRSVAVPELGLGLPHTAFDGRGNAYTSLFLDSQVVKWNIIDEARAYAGEK--INPIKDKLDVHYQPGHLKTVMGETLD	443
Pa.d.	DPRSVAVPELGLGLPHTAFDGRGNAYTSLFLDSQVVKWNIIDEARAYAGEK--VDPIKDKLDVHYQPGHLKTVMGETLD	453
S.m.	QARDTVVAEPELGLGLPHTAYDGKGNAYTTLFIDSQVCKWNIIDEAKRAYAGEK--VDFIRHKLDVHYQPGHNHSMGTQKE	442
R.e.	KLDDAIVAEPELGLGLPHTAFDGRGNAYTTLFIDSQVCKWNIIDAAIKFKHGDKNAKYVVDRLDLQYQPGHVNASQSETVA	459
Ps.n.	ADGKWLVLVLSKFSKDRFLPVGPHLPENDQLIDISGDEMKLVHDGPTFAEPHDAICILVRRDQIKTKK-IYERNDFYFASCRA	465
Ps.s.	ADGKWLVALSKFSKDRFLPVGPHLPENDQLIDISGDEMKLVHDGPTFAEPHDCIMARRDQIKTKK-INDRNDPFFAPVTE	522
Ps.a.	ADGKWLVALSKFSKDRFLPTGPHLPENDQLIDISGDVVKLVHDGPTFAEPHDCIMARRDQIKTKK-INDRNDPFFAPVTE	518
A.c.	AANDWLVLCLCKFSKDRFLVNGVPLKPENDQLIDISGDKMVLVHDGPTFAEPHDAIAVSPSILPNIRSVDRKDPWAEATR	523
Pa.d.	ATNDWLVLCLCKFSKDRFLVNGVPLKPENDQLIDISGDKMVLVHDGPTFAEPHDAIAVHPSILSDIKSVDRNDPMAETRA	533
S.m.	ADGKWLISLNFKFSKDRFLVNGVPLKPENDQLIDISGDEMLVHDNPTFAEPHDAIVHASKINPVH-VNDRDFFADAVA	521
R.e.	ADGKYLAVGCKFSKDRFLPVGPHLPENEQLIDISGQKMLVMDADHPVRGEPHDFIIFKRELVRPKQ-VYALDD--FPLAIK	536
Ps.n.	QAEKDGVTL-ESDNKVIDRGNKVRVYMTSVAPQYGMTEFKVKEGDEVTVVITNLDVMDVTHGFVCMVNHGVSMEISPQQT	544
Ps.s.	MAKKDGINL-DTDNKVIDRGNKVRVYMTSMAPAFGVQEFTVKGDEVTVVITNLDQIEDVSHGFVVMVNHGVSMEISPQQT	601
Ps.a.	MAKKDGINL-EEDNKVIDRGNKVRVYMTSMAPAYGLTEFKVKGNEVTVVITNMDQIEDVSHGFVVMVNHGVSMEISPQQT	597
A.c.	QAEADEVDIDEWTEAVIRDRGNKVRVYMTSVAPSPSQPSFTVKEGDEVTVVITNLDIIDLTHGFTMGNHGVAMEVGPQQT	603
Pa.d.	QAEADGVDIDNWTVEVIRDRGNKVRVYMTSMAPAFGLDFTVKGDEVTVVITNLDIIDLTHGFTMGNYGVAMEIGPQQT	613
S.m.	QAKANDIDL-MVDSEVIRDRGNKVRVYMTSAAPAFGLDFTVKGDEVTVVITNIDEVEDLTHGFCVIGNYVAMEVAPQAT	607
R.e.	DPK-----ESGVRNFRKRVTVKITSQAPAFSLREFKLLKGEVTLITNLDKIEDLTHGFAIPKYNVNFIVNPQET	607
Ps.n.	ASVTFTAGKPGVYVYCNWFCHALHMEMVGRMEVEKKEA	583
Ps.s.	SSITFFVADKPGHLHWYCSWFFCHALHMEMVGRMMVEPA--	638
Ps.a.	SSITFFIADKPGHLHWYCSWFFCHALHMEMVGRMMVEPA--	634
A.c.	SSVTFVAANPGVYVYCNWFCHALHMEMGRMFVEPKGA	642
Pa.d.	SSVTFVAANPGVYVYCNWFCHALHMEMGRMLVEPKGA	652
S.m.	ASVTFKASRPGVYVYCTWFFCHAMHMEMGRMLVEAQGA	639
R.e.	ASVTFVADKPGVFWCYCTHFFCHALHLEMRMIVEA--	643

FIGURE 3: Amino acid sequence comparison of N₂ORs. Comparison was performed using the ClustalX program (43). Labels are as follows: Ps.n., *Pseudomonas nautica* (this work); Ps.s., *Pseudomonas stutzeri* (NCBI sequence number AAA25907); Ps.a., *Pseudomonas aeruginosa* (CAA46381); A.c., *Achromobacter cycloclastes* (CAA75425); Pa.d., *Paracoccus denitrificans* (CAA52798); S.m., *Sinorhizobium meliloti* (ACC44023); and R.e., *Ralstonia eutropha* (CAA46383).

indistinguishable by SDS–PAGE, yielding a band at ~65 kDa and one at ~16 kDa (see below). Mass spectrometric analysis gave a mass of $65\,382 \pm 34$ Da for N₂OR. The molecular mass of the monomer calculated from the amino acid sequence is 65 373 Da. Native molecular mass determination by gel filtration yielded a value of 120 kDa, indicative of a dimer.

Copurification of a 10.3 kDa Peptide with N₂OR. Both forms of N₂OR consistently copurified with a peptide. Its apparent molecular mass, as estimated by SDS–PAGE, was 16 kDa. Electrospray ionization mass spectrometry provided a value of $10\,289.9 \pm 0.4$ kDa. This peptide could not be separated from N₂OR by anion exchange, hydrophobic interaction, adsorption, or gel filtration chromatographies, indicating a strong association between the two proteins, but precipitated upon N₂OR crystallization. Therefore, the spectroscopic and activity data presented in this article were obtained with samples containing this peptide. Amino-terminal sequencing of the 10.3 kDa peptide, following electroblotting, yielded the sequence MKIRPLHDGV-VIKRKNFVIKDASIIGLP. Sequence comparison revealed high homology with proteins of the GroES heat shock chaperonin family (41, 42).

Metal Content of N₂OR. Total copper determination was performed on various batches of both forms of N₂OR. The number of copper atoms found was 10.7 ± 1.7 per dimer, a value slightly higher than those previously reported for this enzyme (3). No significant amounts of other metals were found by plasma emission analysis.

Gene and Protein Sequence. In Figure 2, the partial DNA sequence and the deduced amino acid sequence of *Ps. nautica* N₂OR are presented. Figure 3 shows the comparison of the complete N₂OR amino acid sequence (obtained by N-terminal sequencing, C-terminal sequencing, and translation of the PCR amplification product) with other known N₂OR sequences. Ligands of Cu_Z and Cu_A centers, as determined by X-ray analysis (28), are marked in black and gray, respectively. These amino acids are conserved in all sequences shown. While the coordination sphere of Cu_Z was not predicted or observed before, the ligands of Cu_A were successfully predicted by Zumft (3). Trp563 (identified by an arrow in Figure 3) binds Cu_A through the carbonyl group, which is in accordance with the fact that this residue is not totally conserved (one sequence out of seven shows a histidine instead of a tryptophan).

Crystallographic Data. Blue crystals (Figure 4) grew in about 30 days in the space group *P6*₁, with unit cell dimensions $a = b = 211$ Å, $c = 166$ Å, and 3 dimers per asymmetric unit (55% solvent content, $V_m = 2.73$). The refined three-dimensional model has an R_{factor} of 21.6% ($R_{\text{free}} = 25.0\%$) and contains a dimer of 580×2 residues, 12 copper atoms, and 728 water molecules. The Cu_A center is composed of two copper atoms and is similar to the Cu_A site in subunit II of COX (22–25). The remaining four copper ions are assembled in the Cu_Z center, a novel cluster shaped as a distorted tetrahedron with seven His and three hydroxide ion ligands (Figure 5). A more complete description of the structure is presented elsewhere (28).

Spectroscopic Characterization of Forms A and B of N₂OR. The absorbance spectra of forms A and B of *Ps. nautica* N₂OR are shown in Figure 1. Both forms of the enzyme show absorbance bands in the ranges 540–560 and

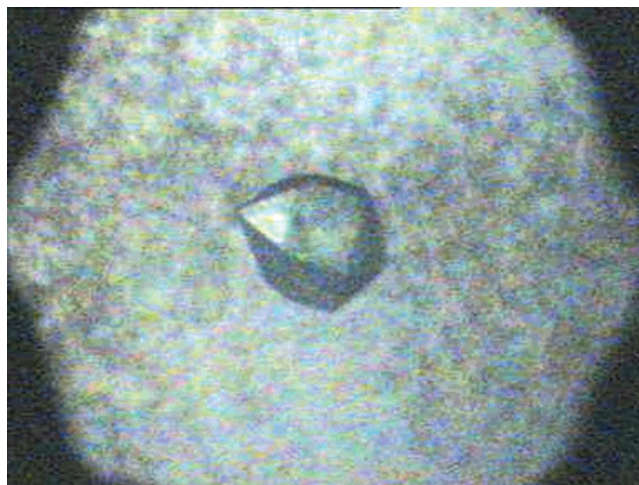


FIGURE 4: Example of a blue crystal of *Ps. nautica* N₂OR used in X-ray diffraction studies.

620–640 nm, but the peak around 540 nm is more intense in form A. In addition, the spectrum of form A shows absorption features at ~480 and ~800 nm. UV/Visible spectroscopy showed that reduction of both forms of the enzyme by sodium dithionite resulted in a decrease in absorption at 540 nm and the bleaching of the 480 and 800 nm features, with a single remaining peak around 640 nm ($\epsilon_{640\text{ nm}} = 7.1 \pm 0.3 \text{ mM}^{-1} \cdot \text{cm}^{-1}$ for the protein dimer) (Figure 1C). This corresponds to the so-called form III of the enzyme, obtained by the addition of excess reductant to native N₂OR (4, 44, 45). Oxidation of either form of N₂OR with potassium ferricyanide resulted in a significant increase in absorption at 480, 540, and 800 nm (data not shown). The UV–visible spectrum of the crystals was characteristic of an almost fully reduced enzyme.

Both enzyme forms were also studied by EPR spectroscopy in the as-purified (Figure 6), dithionite-reduced, and ferricyanide-oxidized states (Figure 7A,B). The spectrum of the fully reduced enzyme could be simulated by assuming a single species with a 4-line hyperfine splitting in the g_z region ($g_x = 2.015$, $A_x = 1.5$ mT, $g_y = 2.071$, $A_y = 2$ mT, $g_z = 2.138$, $A_z = 7$ mT) and line width values of 5.5, 5.0, and 5.5 mT for g_x , g_y , and g_z , respectively. As demonstrated by the oxidized minus reduced difference spectrum (Figure 7C), the fully oxidized spectrum could be simulated by adding, in equal proportions, the simulated signal of the fully reduced enzyme and a Cu_A-like signal exhibiting a 7-line hyperfine splitting in the g_z region ($g_x = g_y = 2.021$, $A_x = A_y = 0$ mT, $g_z = 2.178$, $A_z = 4$ mT) with line width values of 8.0, 8.0, and 3.0 mT for g_x , g_y , and g_z , respectively. The 4-line signal was assigned to Cu_Z by spectral deconvolution of N₂OR spectra at different oxidation states (Figure 7). The spectra of forms A and B, as-purified, were simulated in the same manner assuming that both forms are intermediate redox states between the fully oxidized and the fully reduced form (Figure 6). The proportions of Cu_A (oxidized) and Cu_Z signals used to simulate the various spectra are summarized in Table 1.

The amount of EPR-detectable copper spins was also determined for both forms of the enzyme in different oxidation states (Table 1). For both forms, the EPR spectrum of oxidized N₂OR quantified approximately 2 spins per monomer, whereas the fully reduced form yielded ap-

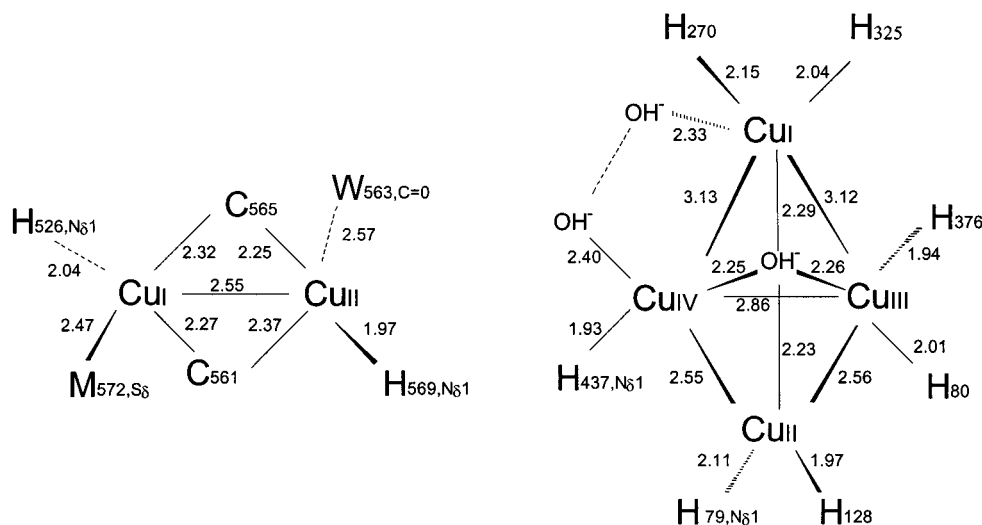


FIGURE 5: Schematic representation of the Cu_A binuclear center and Cu_Z tetranuclear center of *Ps. nautica* N_2OR . Distances were determined from crystallographic data.

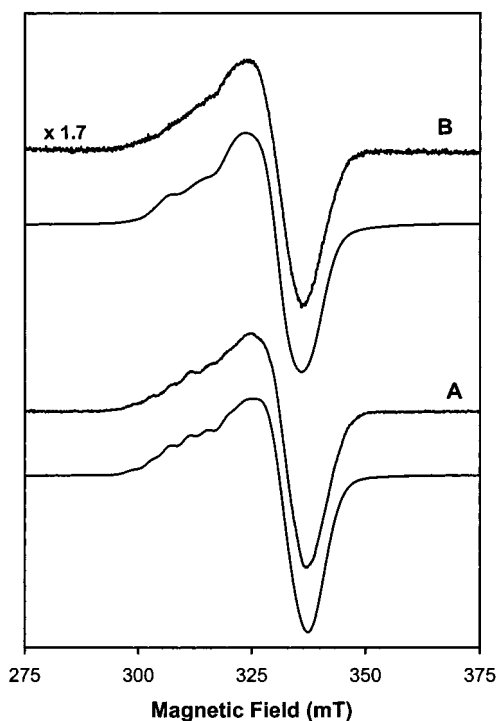


FIGURE 6: EPR spectra of forms A and B of *Ps. nautica* N_2OR , as-purified. (A) Form A, 215 μM enzyme in 160 mM Tris-HCl buffer, pH 7.6, 39 K, microwave power 1.59 mW, modulation 4.05 Gpp, microwave frequency 9.49 GHz. (B) Form B, 267 μM enzyme in 160 mM Tris-HCl buffer, pH 7.6, 35 K, microwave power 5.04 mW, modulation 1.05 Gpp, microwave frequency 9.49 GHz. One scan was run for all spectra, and the gain was 7.1×10^4 . The simulations combine a 4-line and a 7-line signal according to the proportions reported in Table 1.

proximately 1 spin per monomer. The as-purified form A contains about 90% of the spin intensity when compared to the ferricyanide-oxidized state. In the case of form B, only 60% of the spin intensity is present.

Redox Behavior of N_2OR . Redox titrations of N_2OR were followed by EPR spectroscopy. Both forms of the enzyme gave similar results. The data obtained were fitted to a Nernst equation for a one-electron process and a midpoint redox potential of approximately +260 mV (data not shown). No EPR-silent state was ever detected.

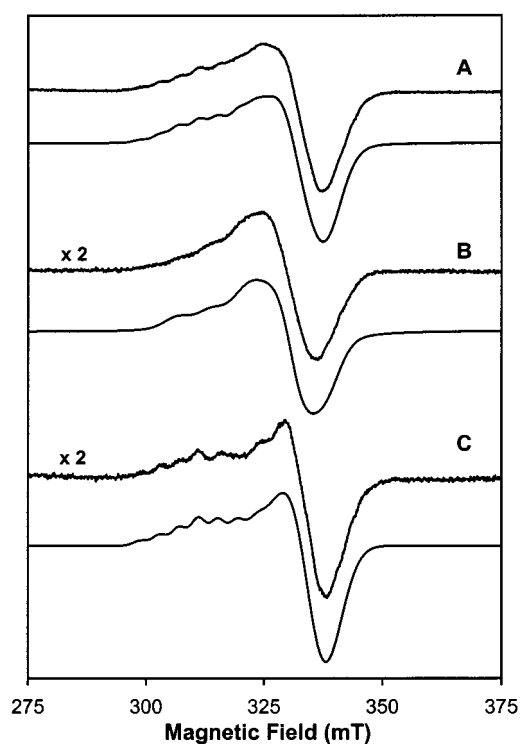


FIGURE 7: EPR spectra of oxidized and reduced N_2OR from *Ps. nautica*. (A) Oxidized enzyme; (B) reduced enzyme; (C) difference spectrum "A minus B". Experimental conditions were 267 μM enzyme in 160 mM Tris-HCl buffer, pH 7.6, 35 K, microwave power 5.05 mW, modulation 1.05 Gpp, microwave frequency 9.49 GHz, 1 scan, gain 7.1×10^4 .

DISCUSSION

The unveiling of the tetranuclear nature of Cu_Z by X-ray crystallography sheds a new light on UV-visible and EPR studies of N_2OR . Our spectroscopic data on the three oxidation states (oxidized, as-purified, and reduced) of forms A and B of *Ps. nautica* N_2OR can only be explained if the two copper centers, Cu_A and Cu_Z , contribute independently to the spectra. We suggest that the main differences observed between the visible spectra of the two forms correspond to a difference in the oxidation state of Cu_A . However, we cannot at present exclude more substantial structural varia-

Table 1: Proportions of Oxidized Cu_A Signal (7 Lines) and Cu_Z Signal (4 Lines) in EPR Spectra

enzyme	oxidized	as-purified	reduced
form A			
spectral deconvolution	0.5 Cu _A /0.5 Cu _Z	0.45 Cu _A /0.55 Cu _Z	1 Cu _Z
spins/6 Cu	2.03	1.89	1.01
form B			
spectral deconvolution	0.5 Cu _A /0.5 Cu _Z	0.08 Cu _A /0.92 Cu _Z	1 Cu _Z
spins/6 Cu	2.2 ^a	1.24	1.05

^a Deduced from spectral deconvolution.

tions. We thus propose the following model: forms A and B of *Ps. nautica* N₂OR are intermediate oxidation states between an oxidized [(Cu^{1.5+}–Cu^{1.5+}) (3Cu¹⁺–Cu²⁺)] state and a one-electron reduced [(Cu¹⁺–Cu¹⁺) (3Cu¹⁺–Cu²⁺)] state. The binuclear Cu_A center, in its oxidized (Cu^{1.5+}–Cu^{1.5+}) state, is responsible for the 7-line signal observed in the EPR spectra of oxidized and as-purified samples, in accordance with the data reported for other N₂ORs (4, 20, 46, 47). The tetranuclear Cu_Z center would then be responsible for the 4-line signal observed in all spectra, suggesting that this center did not undergo any redox transition within the experimental conditions. It should be noted that the spectroscopic characteristics of Cu_Z presented in this work can be explained by two different oxidation schemes: (i) three Cu¹⁺ and one Cu²⁺, or (ii) one Cu¹⁺ and three Cu²⁺. In both cases, the total spin of the tetranuclear cluster will be equal to 1/2, thus explaining the observed EPR signal. However, we favor the first hypothesis because, even at very low redox potential, we could not further reduce the Cu_Z center, which suggests an electron-rich nature for this center. Furthermore, a more reduced state of Cu_Z is in accordance with a putative N₂O reduction mechanism proposed elsewhere (28). While Cu_Z is present in the same, EPR-active, oxidation state in both form A and form B, Cu_A is approximately 85% oxidized in form A and only 20% oxidized in form B, as calculated from data in Table 1.

It has recently been proposed that the catalytic center of N₂OR could not be detected by visible or EPR spectroscopy and that the electron transfer center was solely responsible for the visible absorption bands and EPR signals in all oxidation states of the enzyme (27). According to this model, all observable spectral species, namely, Cu_A, Cu_Z, and Cu_Z* (an altered Cu_Z), correspond to different structural forms of the electron transfer center. This interpretation was mainly based on EPR spin quantitation and deconvolution of LT-MCD spectra. The estimated copper content of the samples used in this study was 3.2–3.9 Cu atoms per monomer. Assuming that this underestimation of copper content was mostly due to an overestimation of protein concentration, and that *Ps. stutzeri* N₂OR indeed contains 6 coppers per monomer, as implied by the conserved histidines in its sequence (Figure 3), we recalculated the number of spins per 6 Cu atoms. For all three samples, the sum of calculated spins for Cu_A, Cu_Z, and Cu_Z* gives 1.90 ± 0.01 spins/6 Cu. This value is in good agreement with our current model, according to which Cu_A and Cu_Z/Cu_Z* are separate centers, with Cu_Z/Cu_Z* being the catalytic site. The main difference with *Ps. nautica* N₂OR is that, in the latter enzyme, the redox potential of the catalytic site must be higher and only the reduced state could be observed. *Ps. stutzeri* N₂OR, however, must have access to three different redox states: [oxidized

Cu_A, oxidized Cu_Z] (“purple” form I), EPR-silent [reduced Cu_A, oxidized Cu_Z], and [reduced Cu_A, reduced Cu_Z] (“blue” form III) (4, 27). One serious discrepancy remains, however, since Farrar et al. (27) established through MCD spectroscopy that all copper centers responsible for the absorption bands in the electronic spectrum were thiolate-coordinated. According to the crystallographic study, only nitrogen atoms (from histidines) and oxygen atoms (H₂O or OH[–]) bind the Cu_Z copper atoms (28). Since it is very likely that the N₂-ORs from *Ps. nautica* and *Ps. stutzeri* share a very similar structure, considering the sequence homology, we must speculate that some absorption bands attributed to a thiolate-coordinated binuclear center may originate from the complex interactions between the four coppers of the Cu_Z center and their ligands. Although our data confirm that the spectroscopically determined Cu_Z and the tetranuclear copper center unveiled by X-ray crystallography are the same, a few questions remain.

Although the two forms of the enzyme were purified under aerobic conditions, there was no indication of the existence of a less active “pink” form, that had been described in other organisms (3). The copurification of N₂OR with a putative chaperonin may have protected the catalytic center from suffering any oxygen-driven alteration. Furthermore, an oxidized state of Cu_Z was not observed, implying that this center possesses an unusually high midpoint redox potential. Such a characteristic could protect Cu_Z from oxidative damage.

The tetranuclear structure of the catalytic site was quite unexpected. There were earlier reports that more than two electrons per dimer were necessary to produce an EPR-active form of the catalytic center (45, 3). This becomes easier to understand, considering the tetranuclearity of the catalytic center, but would suggest that this center may undergo more than one redox transition. At this moment, there is no chemical model that would help us to understand the mechanisms taking place in such a structure. The complex composition of this center may be related to the necessity of activating the rather chemically stable and unreactive N₂O molecule.

With the knowledge at hand, further crystallographic and spectroscopic studies are needed. Currently, efforts are being made to rationalize the involvement of this novel tetranuclear cluster in the catalytic mechanism of nitrous oxide reduction.

ACKNOWLEDGMENT

Dr. René Toci (CNRS, Marseille) is acknowledged for providing *Pseudomonas nautica* cells. We gratefully acknowledge Gordon Leonard and Sean McSweeney for assistance during data collection (BM14 and ID14-4, ESRF), and Thomas Ursby (IBS-Grenoble) for assistance in the recording of crystal spectra.

REFERENCES

- Hochstein, L. I. (1988) *Annu. Rev. Microbiol.* 42, 231–261.
- Bell, L. C., and Ferguson, S. J. (1991) *Biochem. J.* 273, 423–427.
- Zumft, W. G. (1997) *Microbiol. Mol. Biol. Rev.* 61, 533–616.
- Coyle, C. L., Zumft, W. G., Kroneck, P. M. H., Körner, H., and Jakob, W. (1985) *Eur. J. Biochem.* 153, 459–467.

5. McEwan, A. G., Greenfield, A. J., Wetzstein, H. G., Jackson, J. B., and Ferguson, S. J. (1985) *J. Bacteriol.* **164**, 823–830.
6. Michalski, W. P., Hein, D. H., and Nicholas, D. J. D. (1986) *Biochim. Biophys. Acta* **872**, 50–60.
7. Snyder, S. W., and Hollocher, T. C. (1987) *J. Biol. Chem.* **262**, 6515–6525.
8. Teraguchi, S., and Hollocher, T. C. (1989) *J. Biol. Chem.* **264**, 1972–1979.
9. Hulse, C. L., and Averill, B. A. (1990) *Biochem. Biophys. Res. Commun.* **166**, 729–735.
10. SooHoo, C. K., and Hollocher, T. C. (1991) *J. Biol. Chem.* **266**, 2203–2209.
11. Berks, B. C., Baratta, D., Richardson, D. J., and Ferguson, S. J. (1993) *Eur. J. Biochem.* **212**, 467–476.
12. Hole, U. H., Vollack, K. U., Zumft, W. G., Eisenmann, E., Siddiqui, R. A., Friedrich, B., and Kroneck, P. M. H. (1996) *Arch. Microbiol.* **165**, 55–61.
13. Ferretti, S., Grossmann, J. G., Hasnain, S. S., Eady, R. R., and Smith, B. E. (1999) *Eur. J. Biochem.* **259**, 651–659.
14. Jones, A. M., Hollocher, T. C., and Knowles, R. (1992) *FEMS Microbiol. Lett.* **92**, 205–209.
15. Chan, S. I., and Li, P. M. (1990) *Biochemistry* **29**, 1–12.
16. Kroneck, P. M. H., Antholine, W. A., Riester, J., and Zumft, W. G. (1988) *FEBS Lett.* **242**, 70–74.
17. Scott, R. A., Zumft, W. G., Coyle, C. L., and Dooley, D. M. (1989) *Proc. Natl. Acad. Sci. U.S.A.* **86**, 4082–4086.
18. Kroneck, P. M. H., Antholine, W. A., Riester, J., and Zumft, W. G. (1989) *FEBS Lett.* **248**, 212–213.
19. Kroneck, P. M. H., Antholine, W. E., Kastrau, D. H. W., Buse, G., Steffens, G. C. M., and Zumft, W. G. (1990) *FEBS Lett.* **268**, 274–276.
20. Antholine, W. E., Kastrau, D. H. W., Steffens, G. C. M., Buse, G., Zumft, W. G., and Kroneck, P. M. H. (1992) *Eur. J. Biochem.* **209**, 875–881.
21. Kelly, M., Lappalainen, P., Talbo, G., Haltia, T., van der Oost, J., and Saraste, M. (1993) *J. Biol. Chem.* **268**, 16781–16787.
22. Iwata, S., Ostermeier, C., Ludwig, B., and Michel, H. (1995) *Nature* **376**, 660–669.
23. Tsukihara, T., Aoyama, H., Yamashita, E., Tomizaki, T., Yamaguchi, H., Shinzawa-Itoh, K., Nakashima, R., Yaono, R., and Yoshikawa, S. (1995) *Science* **269**, 1069–1074.
24. Wilmanns, M., Lappalainen, P., Kelly, M., Sauer-Eriksson, E., and Saraste, M. (1995) *Proc. Natl. Acad. Sci. U.S.A.* **92**, 11955–11959.
25. Tsukihara, T., Aoyama, H., Yamashita, E., Tomizaki, T., Yamaguchi, H., Shinzawa-Itoh, K., Nakashima, R., Yaono, R., and Yoshikawa, S. (1996) *Science* **272**, 1136–1144.
26. Beinert, H. (1997) *Eur. J. Biochem.* **245**, 521–532.
27. Farrar, J. A., Zumft, W. G., and Thomson, A. J. (1998) *Proc. Natl. Acad. Sci. U.S.A.* **95**, 9891–9896.
28. Brown, K., Prudêncio, M., Pereira, A. S., Besson, S., Moura, J. J., Moura, I., Tegoni, M., and Cambillau, C. (2000) *Nat. Struct. Biol.* (in press).
29. Spröer, C., Lang, E., Hobeck, P., Burghardt, J., Stackebrandt, E., and Tindall, B. J. (1998) *Int. J. Syst. Bacteriol.* **48**, 1445–1448.
30. Baumann, P., and Baumann, L. (1986) in *The Prokaryotes. A Handbook on Habitats, Isolation and Identification of Bacteria* (Starr, M. P., Stolp, H., Trüper, H. G., Balows, A., and Schlegel, H. G., Eds.) Vol. 2, pp 1302–1331, Springer-Verlag, New York.
31. Starkey, R. L. (1938) *Arch. Mikrobiol.* **8**, 268–304.
32. Laemmli, U. K. (1970) *Nature* **227**, 680–685.
33. Lowry, O. H., Rosebrough, N. J., Farr, A. L., and Randall, R. J. (1951) *J. Biol. Chem.* **193**, 265–275.
34. Poillon, W. N., and Dawson, C. R. (1963) *Biochim. Biophys. Acta* **77**, 27–36.
35. Kristjansson, J. K., and Hollocher, T. C. (1980) *J. Biol. Chem.* **255**, 704–707.
36. Boyd, V. L., Bozzini, M., Zon, G., Noble, R. L., and Mattaliano, B. (1992) *Anal. Biochem.* **206**, 344–352.
37. Bozzini, M. L., Zhao, J., Yuan, P. M., Ciolek, D., Pan, Y. C., Horton, J., Marshak, D. R., and Boyd, V. L. (1995) in *Techniques in Protein Chemistry VI* (Crabb, J. W., Ed.) pp 229–237, Academic Press, New York.
38. Hu, W., Van Driessche, G., Devreese, B., Goodhew, C. F., McGinnity, D. F., Saunders, N., Fülöp, V., Pettigrew, G. W., and Van Beeumen, J. J. (1997) *Biochemistry* **36**, 7958–7966.
39. Strauss, W. M. (1998) in *Current Protocols in Molecular Biology* (Ausubel, F. M., Brent, R., Kingston, R. E., Moore, D. D., Seidman, J. G., Smith, J. A., and Struhl, K., Eds.) pp 2.4.1–2.4.2, Greene Publishing and Wiley-Interscience, New York.
40. Sambrook, J., Fritsch, E. F., and Maniatis, T. (1989) *Molecular Cloning: A Laboratory Manual*, 2nd ed., Cold Spring Harbor Laboratory Press, Cold Spring Harbor, NY.
41. Braig, K. (1998) *Curr. Opin. Struct. Biol.* **8**, 159–165.
42. Sipos, A., Klocke, M., and Frosch, M. (1991) *Infect. Immun.* **59**, 3219–3226.
43. Thompson, J. D., Gibson, T. J., Plewniak, F., Jeanmougin, F., and Higgins, D. G. (1997) *Nucleic Acids Res.* **25**, 4876–4882.
44. Jin, H., Thomann, H., Coyle, C. L., and Zumft, W. G. (1989) *J. Am. Chem. Soc.* **111**, 4262–4269.
45. Riester, J., Zumft, W. G., and Kroneck, P. M. H. (1989) *Eur. J. Biochem.* **178**, 751–762.
46. SooHoo, C. K., Hollocher, T. C., Kolodziej, A. F., Orme-Johnson, W. H., and Bunker, G. (1991) *J. Biol. Chem.* **266**, 2210–2218.
47. Zhang, C. S., Hollocher, T. C., Kolodziej, A. F., and Orme-Johnson, W. H. (1991) *J. Biol. Chem.* **266**, 2199–2202.

BI9926328